Leptoquark search at the Forward Physics Facility

Kingman Cheung,[1,2,3] Thong T. Q. Nguyen,[4] and C. J. Ouseph[1,2]

[1]*Department of Physics, National Tsing Hua University, Hsinchu 30013, Taiwan*
[2]*Center for Theory and Computation, National Tsing Hua University, Hsinchu 30013, Taiwan*
[3]*Division of Quantum Phases and Devices, School of Physics, Konkuk University, Seoul 143-701, Republic of Korea*
[4]*Insitute of Physics, Academia Sinica, Nangang, Taipei 11529, Taiwan*

(Received 21 April 2023; accepted 24 July 2023; published 14 August 2023)

In this study, we calculate the sensitivity reach on the vector leptoquark (LQ) U_1 at the experiments proposed in the Forward Physics Facility (FPF), including FASERν, FASERν2, FLArE (10 tons), and FLArE (100 tons) using the neutrino-nucleon scattering ($\nu N \to \nu N'$ and $\nu N \to lN'$). We cover a wide mass range of 10^{-3} GeV $\leq M_{\rm LQ} \leq 10^4$ GeV. The new result shows that the FLArE (100 tons) offers the best sensitivity to the LQ model. The sensitivity curves for all the experiments follow a similar pattern with weakened sensitivities with the increment of the LQ mass. We combine the sensitivities obtained from the neutral- and charged-current interactions of the neutrinos.

DOI: 10.1103/PhysRevD.108.036014

I. INTRODUCTION

Hunting for new physics beyond the standard model (SM) is one of the major goals at various experiments in high-energy and intensity frontiers. While the high-energy frontier has not found anything other than the discovery of the Higgs boson, the precision frontier, on the other hand, seemed to show some surprising results on a number of B meson decays, and the muon anomalous magnetic dipole moment, although more data are needed to confirm.

The discrepancies existed between the SM predictions and the experimental results for the flavor-changing neutral current rare decays of B mesons in $b \to s\ell^+\ell^-$, in particular, the lepton-flavor universality violation in $B \to K$ transition observed by LHCb, expressed in terms of R_K and R_{K^*}:

$$R_K = \frac{\mathrm{BR}(B \to K\mu^+\mu^-)}{\mathrm{BR}(B \to Ke^+e^-)}, \quad R_{K*} = \frac{\mathrm{BR}(B \to K^*\mu^+\mu^-)}{\mathrm{BR}(B \to K^*e^+e^-)}. \quad (1)$$

[1] Nevertheless, the anomalies have faded away in the most recent measurements [3], which showed consistency with the SM predictions:

$$R_K = \begin{cases} 0.994^{+0.090}_{-0.082}(\mathrm{stat})^{+0.029}_{-0.027}(\mathrm{syst}) & \mathrm{low} - q^2, \\ 0.949^{+0.042}_{-0.041}(\mathrm{stat})^{+0.036}_{-0.035}(\mathrm{syst}) & \mathrm{central} - q^2, \end{cases} \quad (4)$$

$$R_{K^*} = \begin{cases} 0.927^{+0.042}_{-0.041}(\mathrm{stat})^{+0.022}_{-0.022}(\mathrm{syst}) & \mathrm{low} - q^2, \\ 1.027^{+0.072}_{-0.068}(\mathrm{stat})^{+0.027}_{-0.026}(\mathrm{syst}) & \mathrm{central} - q^2. \end{cases} \quad (5)$$

Another set of observables related to the short-distance process $b \to c\ell\nu$ are [4]

[1]The discrepancies between the SM predictions and the experimental results for the flavor-changing neutral current rare decays of B mesons in $b \to s\ell^+\ell^-$ were as large as 3σ with the measurements [1,2]

$$R_K = 0.846^{+0.042+0.013}_{-0.039-0.012}, \quad \text{for } 1.1\ \mathrm{GeV}^2 < q^2 < 6\ \mathrm{GeV}^2, \quad (2)$$

$$R_{K^*} = \begin{cases} 0.66^{+0.11}_{-0.07} \pm 0.03 & 0.045\ \mathrm{GeV}^2 < q^2 < 1.1\ \mathrm{GeV}^2, \\ 0.69^{+0.11}_{-0.07} \pm 0.05 & 1.1\ \mathrm{GeV}^2 < q^2 < 6.0\ \mathrm{GeV}^2. \end{cases} \quad (3)$$

$$R_D = \frac{\mathrm{BR}(B \to D\tau\nu)}{\mathrm{BR}(B \to D\ell\nu)} = 0.340 \pm 0.027 \pm 0.013,$$
$$R_{D^*} = \frac{\mathrm{BR}(B \to D^*\tau\nu)}{\mathrm{BR}(B \to D^*\ell\nu)} = 0.295 \pm 0.011 \pm 0.008, \quad (6)$$

which still showed discrepancies from the SM.

Another long-standing experimental anomaly is the muon anomalous moment (also known as $g-2$). The most recent muon $g-2$ measurement was performed by the E989 experiment at Fermilab, which reported the new result [5],

$$\Delta a_\mu = (25.1 \pm 5.9) \times 10^{-10}, \quad (7)$$

which deviates at the level of 4.2σ from the known SM predictions before the recent lattice results. The recent lattice results [6,7] made substantial improvements in hadronic contributions to $g-2$ such that the deviation of the experimental result only stands at about the $1-2\sigma$ level.

Leptoquark (LQ) models were suggested to explain some or all of the above anomalies. Especially, it was shown in Refs. [8–10] that the isosinglet vector LQ U_1 can explain both R_{K,K^*} and R_{D,D^*}, and in Ref. [11] that the isodoublet vector LQ V_2 provides a viable solution to R_{K,K^*}, R_{D,D^*}, and muon $g-2$. On the other hand, other LQ models can only explain one or some of the anomalies, unless with more than 1 leptoquark. In this work, we do not concern ourselves with the second- and third-generation quark couplings, nor do we assume any flavor symmetries. We only consider the first-generation quark couplings as they are more relevant in neutrino-nucleon scattering. Our results will not reflect any constraints on the second or third-generation couplings.

Such LQs have been searched at the LHC with strong limits on the LQ mass via leptoquark pair production. The mass limits depend on the decay channels of the LQs. Nevertheless, such decays often make use of the decay into a quark and a charged lepton. When the LQ decays into a quark plus a neutrino, the limits are much weakened.

In this work, we investigate the effects of LQs via neutrino-nucleon scattering at the FASERν, and the future FASER2ν and FLArE experiments. The ultimate plan is to have a Forward Physics Facility (FPF) [12], which can house a number of such experiments. FASERν is indeed running and taking data [13,14]. Such experiments use the energetic neutrinos produced by the decays of mesons (e.g., pions, kaons) from the interaction point of the ATLAS experiment. The most distinct feature is that the energy range can be as high as TeV, which provides an unprecedented energy scale of studying neutrino-nucleon and neutrino-electron scattering.

We focus on the isosinglet vector LQ U_1, though the results can be easily adapted to the isodoublet vector LQ V_2. An interesting feature of the LQ is that it can enhance both the charged- and neutral-current interactions, so it can give better sensitivities than the Z' interactions, which only enhance the neutral-current interactions [15]. We calculate both the charged- and neutral-current scattering via the LQ and obtain the sensitivities that one can obtain at FASERν, FASER2ν, and FLArE.

The organization is as follows. In the next section, we describe the interactions of the LQ that are relevant to our study. In Sec. III, we present the numerical results and the sensitivity reach at various FPF experiments.

Note that we are exploring very light leptoquarks with small couplings to quarks and leptons. Nevertheless, the relevant couplings in our study are those of LQ with the first-generation quarks (u and d) in the νN scattering, while those explaining the B anomalies concern mostly the third and second generations. Thus, we do not restrict the LQ couplings to those obtained in B anomalies.

II. THEORETICAL SETUP

A. Leptoquark model

Leptoquarks are predicted in many grand unified theories, which couple to both quarks and leptons. It was shown in Ref. [10] that the singlet vector leptoquark $U(1)$ with the SM quantum numbers ($\mathbf{3}$, $\mathbf{1}$, $2/3$) can explain both R_{K,K^*} and R_{D,D^*} anomalies. The Yukawa interactions for U_1 can be written as [16–18]

$$\mathcal{L}_{U_1} = \frac{g_U}{\sqrt{2}}\left[U_1^\mu(\beta_L^{ij}\bar{q}_L^i\gamma_\mu l_L^j + \beta_R^{ij}\bar{d}_R^i\gamma_\mu l_R^j) + \mathrm{H.c.}\right], \quad (8)$$

where q_L, l_L, d_R, l_R denote the quark doublet, lepton doublet, down-type quark singlet, and lepton singlet, respectively. Here i and j denote the generation indices, and $\beta_{L/R}^{ij}$ allow for generation mixing, and g_U is the overall coupling strength.

We used the vector leptoquark models from Refs. [16–18], which can be accessed from the FeynRules model database ([19]). We choose β^{2j} and β^{3j} (for $j = 1, 2, 3$) to be zero, such that the flavor-changing neutral currents among the first, the second, and the third-generation quarks are avoided. Also, only the first-generation-quark couplings β^{1j} are relevant to our study. Such choices may give rise to lepton-flavor changing processes, e.g., $\tau \to \mu$ decays, but, however, we expect them to be negligible, as no second- or third-generation quarks are involved.

Note that although we use the leptoquark U_1 in our study, the cases with other leptoquarks would give results with similar orders of magnitude on the sensitivity reach. Unlike scalar leptoquarks, vector leptoquarks must have some extra degrees of freedom due to the UV sensitivity of the loop [20], where an example of UV completion was given.

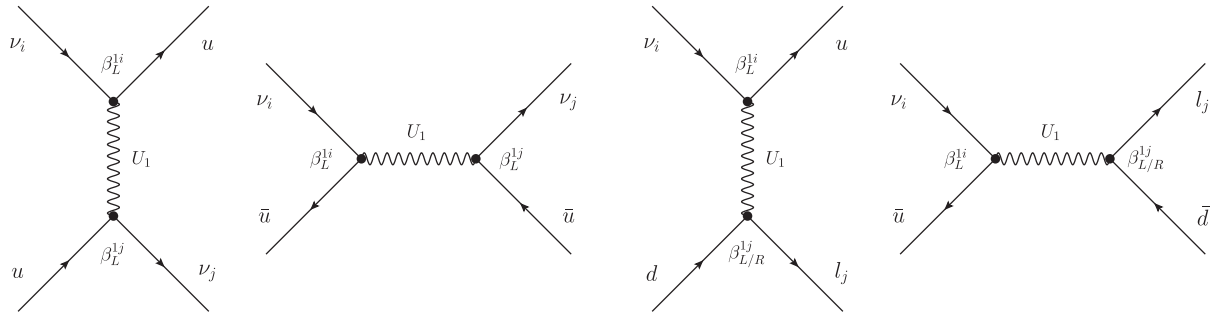

(a) Neutral Current (b) Charged Current

FIG. 1. Contributing Feynman diagrams between the neutrino and the first-generation quark/antiquark through a vector-leptoquark exchange. The diagrams for antineutrinos and $d/\bar{d}$ particles can be similarly written down.

B. Neutrino-nucleon scattering via leptoquarks

In neutrino experiments, the leptoquark U_1 can participate in the neutral- and charged-current scattering between the incoming neutrino and the quark from protons or neutrons (nucleons) of the detector materials:

(1) Neutral current (NC): $\nu_i + N \to \nu_j + N'$.
(2) Charged current (CC): $\nu_i + N \to l_j + N'$.

The contributing Feynman diagrams for the neutrino-quark scattering processes are shown in Fig. 1. The amplitude for the NC scattering shown in Fig. 1 is given by, in the limit of heavy LQ mass,

$$\begin{aligned} i\mathcal{M}_{NC} &= i\frac{g_U^2}{2M_{U_1}^2}\beta_L^{1i}\beta_L^{1j}(\overline{u_L}\gamma^\mu\nu_{iL})(\overline{\nu_{jL}}\gamma_\mu u_L) \\ &= -i\frac{g_U^2}{2M_{U_1}^2}\beta_L^{1i}\beta_L^{1j}(\overline{u_L}\gamma^\mu u_L)(\overline{\nu_{jL}}\gamma_\mu\nu_{iL}), \end{aligned} \tag{9}$$

where the second line explicitly shows the NC scattering, which is obtained by the Fierz transformation. On the other hand, the CC scattering for $\nu_{iL}d_{L/R} \to u_L e_{L/R}$ can proceed via the left- and right-handed couplings, of which the amplitude is given by, in the limit of heavy LQ mass,

$$\begin{aligned} i\mathcal{M}_{CC} &= i\frac{g_U^2}{2M_{U_1}^2}\beta_L^{1i}(\overline{u_L}\gamma^\mu\nu_{iL})(\beta_L^{1j}\overline{e_{jL}}\gamma_\mu d_L + \beta_R^{1j}\overline{e_{jR}}\gamma_\mu d_R) \\ &= i\frac{g_U^2}{2M_{U_1}^2}\beta_L^{1i}[-\beta_L^{1j}(\overline{u_L}\gamma^\mu d_L)(\overline{e_{jL}}\gamma_\mu\nu_{iL}) \\ &\quad + 2\beta_R^{1j}(\overline{u_L}d_R)(\overline{e_{jR}}\nu_{iL})], \end{aligned} \tag{10}$$

where the CC scattering is demonstrated explicitly in the second line, which is obtained by the Fierz transformation.

Since we consider fixed-target scattering between neutrinos/antineutrinos and nucleon (detector), we neglect the effect of gluon-leptoquark interaction, and also the interaction between the leptoquark and photon or neutral Z boson. Note that neutrinos will not scatter with electrons via the LQ U_1, but, on the other hand, antineutrinos do scatter with electrons via the LQ U_1. This can be distinguished from the neutrino-nucleon scattering by the recoil nucleus.

The proposed FPF is set to be placed at several hundred meters from the ATLAS interaction point, shielded by concrete and rock [21]. This FPF will house a number of experiments that will explore processes of the SM, as well as look for any physics beyond the Standard Model (BSM) [15,22–49]. Such experiments are necessitated due to the high energy collisions at the High-Luminosity Large Hadron Collider (HL LHC), which generates a large number of particles along the beam collision axis, beyond the scope of current LHC experiments.

A plethora of hadrons, such as pions, kaons, and more, are known to be produced along the beam direction. As these hadrons decay during the flight, they produce neutrinos of all three flavors at very high energies up to a few TeV. Studies have revealed that muon neutrinos are primarily created from charged-pion decays; electron neutrinos arise from hyperon, kaon, and D-meson decays; and tau neutrinos stem from D_s meson decays. These neutrinos have an average energy ranging from 600 GeV to 1 TeV, comprising a wide energy range for each of the three neutrino flavors.

The following neutrino detectors are either operational or proposed for the far forward region of the LHC:

(1) FASERν: A targeted mass located at the front of the FASER main detector in a narrow trench (illustrated in Fig. 2 of Ref. [50]), that is made from 1.2 tons of tungsten with the size of 25 cm × 30 cm × 1.1 m.
(2) FASERν2: a detector, which is designed as a much large successor to FASERν, has a total volume of tungsten target of 50 cm × 50 cm × 8 m, so the total mass is 20 tons. A full description of the detectors and their requirements can be found in Ref. [12].
(3) FLArE: a proposed liquid argon time projection chamber (LArTPC) with an active volume of 10 tons (FLArE-10) to 100 tons (FLArE-100).

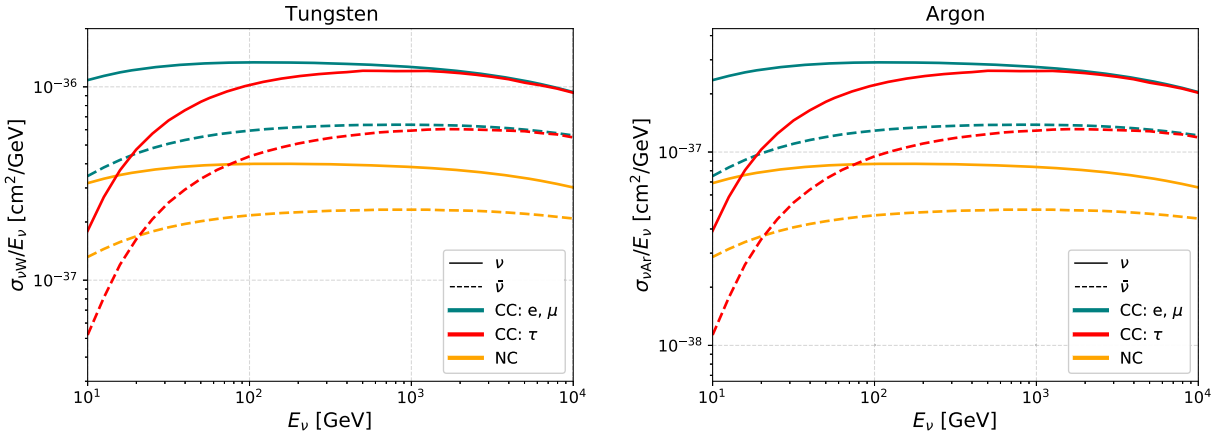

FIG. 2. The SM cross sections per neutrino energy for the scattering of (anti)neutrinos with tungsten (left panel) and with argon (right panel). Neutrino and antineutrino are separately shown. NC and CC for (e, μ) and τ are shown.

To estimate the number of events that occur inside these detectors, we calculate the scattering cross sections of neutrinos/antineutrinos with the nucleus of the detector materials. At nucleon level, the cross section is related to the neutrino/antineutrino parton cross section as

$$\sigma_{\nu N} = \sum_i \int_0^1 dx_2 f(x_2, Q_2) \sigma_{\nu q_i}, \tag{11}$$

where $f(x_2, Q_2)$ is the parton distribution function (PDF) of q_i inside the proton or neutron. This PDF depends on the momentum fraction x_2 and the factorization scale Q_2, which we have chosen $Q_2 = m_Z$. We use the datasets from the LHAPDF library in Ref. [51].

We show the SM NC and CC cross sections for neutrinos and antineutrinos in each detector's material in Fig. 2. In general, the neutrino gives a larger cross section than the antineutrino, and the CC cross section is larger than the NC one. Note that the CC tau-neutrino and tau-anti-neutrino have lower cross sections than corresponding ones of electron and muon, because of a higher threshold to produce a tau lepton. The effects of leptoquark interactions are shown for NC and CC scattering in Figs. 3 and 4, respectively, for various leptoquark masses 10–1000 GeV. Here we have set g_U and $\beta^{1j}_{L/R} = 1$.

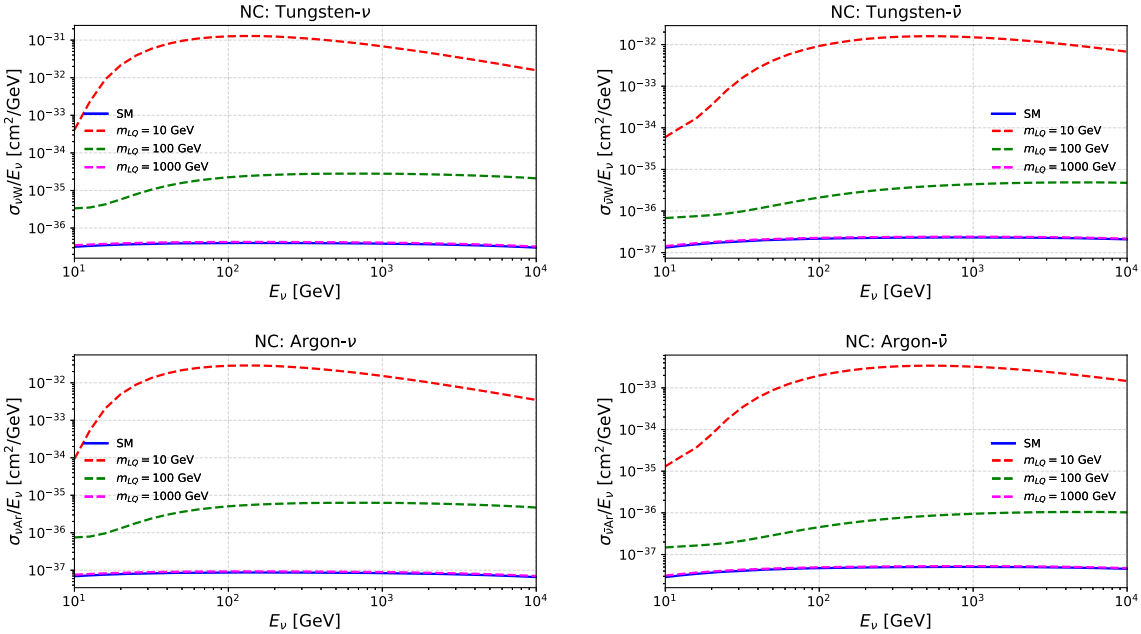

FIG. 3. Neutral-current (NC) scattering cross sections per neutrino energy versus the neutrino energy for both tungsten and argon targets. We show the results for the SM and for various leptoquark masses, and set all the couplings $g_U = \beta^{1j} = 1$.

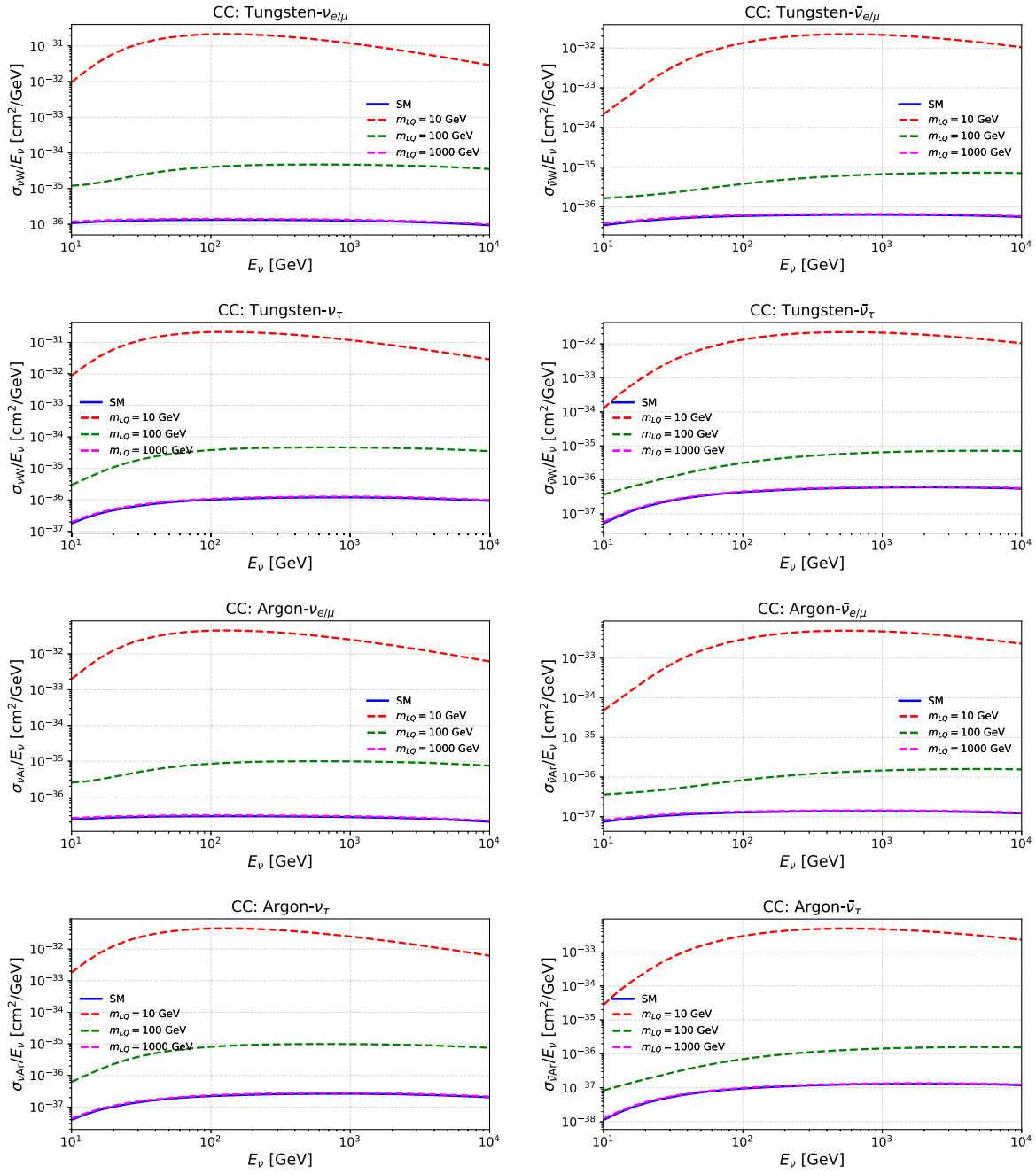

FIG. 4. Charged current (CC) scattering cross sections per neutrino energy. All the details are similar to Fig. 3.

To calculate the CC and NC cross sections for each process, we use the U_1 leptoquark model file, which is a modified version of Refs. [16–18], and input it to FeynRules to generate a model file for use in MadGraph5_aMC@NLO (Refs. [52,53]). To match the results from Ref. [50], we used the same NNPDF3.1NNLO PDF (Ref. [54]).

A discussion on the background coming from neutrino-electron or antineutrino-electron scattering is in order here. We found that the leptoquark exchange is not possible in the neutrino-electron scattering, while it is possible to participate in antineutrino-electron scattering $\bar{\nu}e^- \to \bar{u}d$ via the t-channel LQ exchange (Fig. 5). Nevertheless, the nucleus remains intact in this case. We can make use of the recoiled nucleus to distinguish the signal from this background. However, the hadronic part in the CC ν-nucleon scattereing may not be fully identified with 100% efficiency. Therefore, whether this reducible background can be completely removed depends on the experimental setup and resolution. We take into account this background uncertainty by including it into the systematic uncertainty in the estimation of sensitivities.

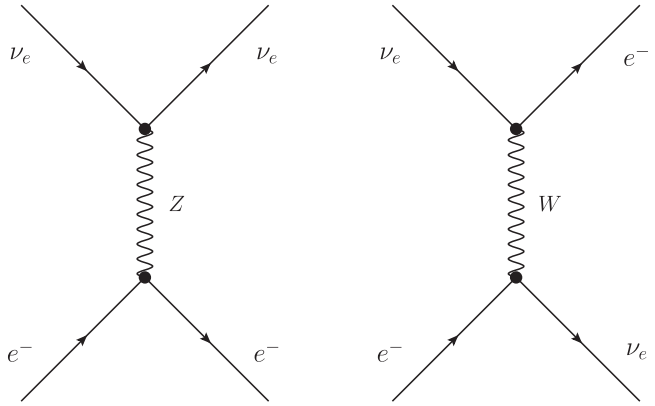

FIG. 5. Feynman diagrams for the neutrino-electron in tungsten/argon detectors, as the SM background for our process.

Besides cross sections, we have to take into account the neutrino and antineutrino fluxes to calculate the number of events. These fluxes are measured and distinguishable for each (anti)neutrino flavor in FASERν, FASERν2, and FLArE detectors. We used the fluxes calculated in Ref. [50] for FASERν, and the simulated fluxes for FASERν2, FLArE 10 and 100 tons from Ref. [12]. The uncertainties in the incoming (anti)neutrino fluxes were studied in Ref. [55]. The electron-neutrino flux has less than 10% uncertainty up to 0.8 TeV, while the dominated muon neutrino flux has less than 10% uncertainty up to 1 TeV, and the tau-neutrino flux has less than 10% uncertainty up to 0.3–0.4 TeV. Overall, the uncertainties are within a factor of 2. Such uncertainties will propagate to the event rate predictions of order a few percent up to 20%, so we can include them in the systematic uncertainties. We take into account the uncertainties due to the hadronic efficiencies and the incoming neutrino flux by including them into the systematic uncertainties of order 10% of the SM predictions [12], which we expect to go down with more intensive studies.

III. SENSITIVITY ON THE VECTOR LEPTOQUARK U_1

Using the neutrino fluxes [12,50] and the cross sections calculated for both the SM and the leptoquark model, we show the total number of events for various FPF detectors in Fig. 6. Once we obtain the predicted number of events $N_{\rm BSM}$ for the leptoquark model as a function of the coupling, and that for the SM $N_{\rm SM}$, we estimate the sensitivity reach in the parameter space (g_U or $g_U \times \beta^{1j}$ vs M_{LQ}) of the model. Here we have taken the statistical error to be $\sqrt{N_{\rm BSM}}$ and the systematic uncertainty to be $\sigma = 10\%$ of the normalization of the SM predictions. For all three generations of neutrinos, we defined the measure of χ^2 as a function of the coupling $g_{\rm BSM} = g_U$ or $g_U \times \beta^{1j}$ and a nuisance parameter α as follows Ref. [56]:

$$\chi^2(g_{\rm BSM},\alpha) = \min_{\alpha}\left[\frac{[N^{\nu_e}_{\rm BSM} - (1+\alpha)N^{\nu_e}_{\rm SM}]^2}{N^{\nu_e}_{\rm BSM}} + \frac{[N^{\nu_\mu}_{\rm BSM} - (1+\alpha)N^{\nu_\mu}_{\rm SM}]^2}{N^{\nu_\mu}_{\rm BSM}} + \frac{[N^{\nu_\tau}_{\rm BSM} - (1+\alpha)N^{\nu_\tau}_{\rm SM}]^2}{N^{\nu_\tau}_{\rm BSM}} + \left(\frac{\alpha}{\sigma}\right)^2\right], \quad (12)$$

where $N_{\rm BSM} = N_{\rm LQ} + N_{\rm Int} + N_{\rm SM}$ and the minimization is over the nuisance parameter α. Here $N_{\rm LQ}$ is the number of events that only comes from leptoquark contribution, while $N_{\rm Int}$ is the interference term between the leptoquark and the SM. We have treated the systematic uncertainties the same for each neutrino flavor and used only one nuisance parameter α. For the following analysis results, we choose $\chi^2 = 3.84$ for the 95% confidence level (CL) sensitivity reach.

In the NC scattering, we cannot distinguish the neutrino flavor, and the leptoquark couplings $\beta^{1j}_{L/R}$ allow lepton-flavor changing, so we include all three flavors of neutrino in the final state. On the other hand, we can identify the

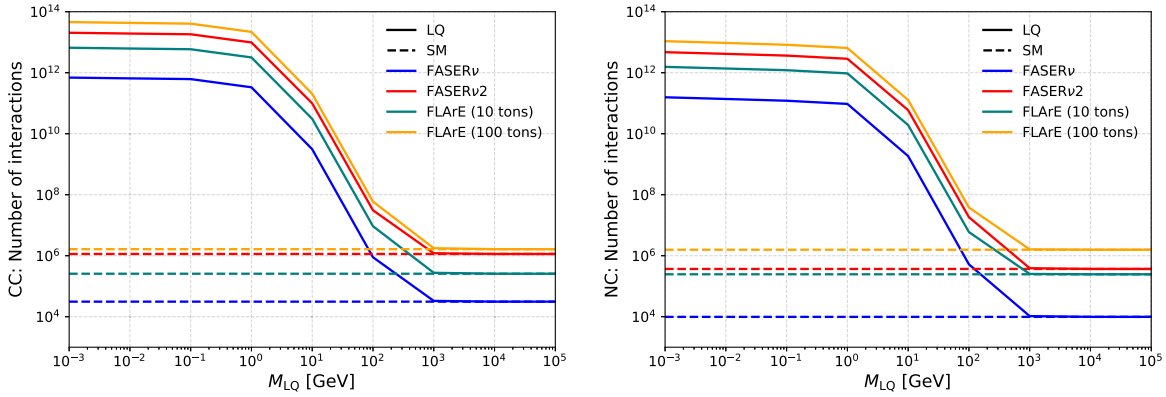

FIG. 6. Number of events for the FPF detectors versus the leptoquark mass. We set all the couplings $g_U = \beta^{1j} = 1.0$. Here the solid lines are for the leptoquark while the dashed lines are for the SM.

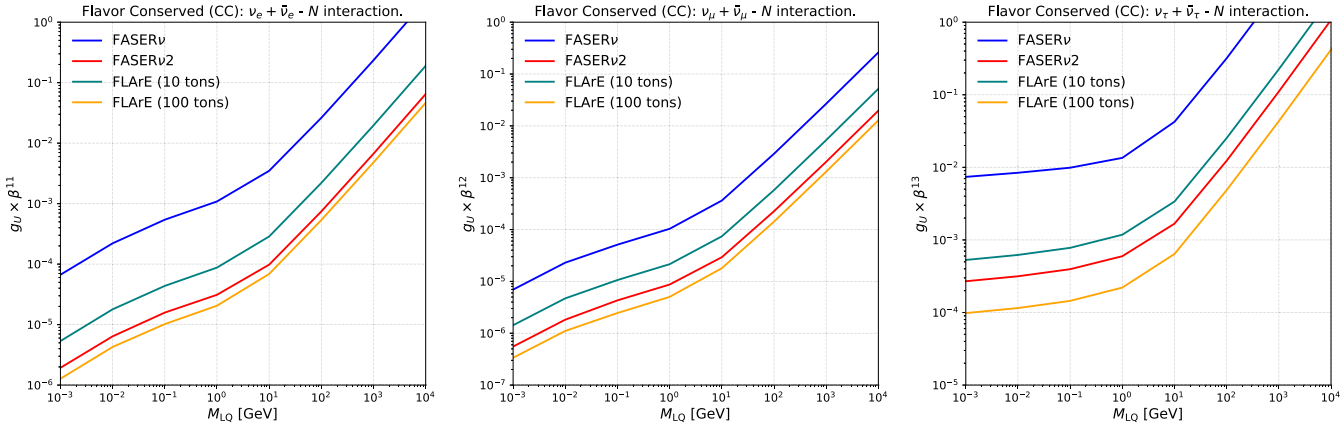

FIG. 7. 95% CL sensitivity curves on $g_U \times \beta^{1j}$, with $j = 1$ (left), $j = 2$ (middle), and $j = 3$ (right) for the CC scattering. We do not include the lepton-flavor-changing processes in our calculations, i.e., only $\nu_i + N \to l_i + N'$ are considered.

outgoing charged leptons in the final state in the CC scattering. Since we know the flavor of the incoming neutrino fluxes, we consider only the lepton-flavor-conserving processes. Thus, we can actually obtain the sensitivity β^{1j} for each j neutrino generation.

The sensitivities obtained using the CC scattering for each neutrino flavor are shown in Fig. 7. Comparing the sensitivity of each coupling $g_U \times \beta^{1j}$, we can see the coupling for muon (second generation) has the best sensitivity at the FPF detectors since the muon (anti) neutrino flux is the largest, while the sensitivity for the tau (anti)neutrino is the least as the tau neutrino flux is the smallest. In Fig. 7, we can also see that FLArE (100 tons) has the best sensitivity, followed by FASERν2, FLArE (10 tons), and FASERν. Next, we include the lepton-flavor-changing processes by including all leptons or antileptons in the CC final state. These lepton-flavor-changing contributions increase the number of signal events. For simplicity we take all $\beta^{1j}_{L/R}$ equal to 1. Thus, we obtain the sensitivities on g_U.

For NC scattering we include all (anti)neutrino flavors in the final state, and thus we can obtain the sensitivities on g_U. We show the results for FASERν, FASERν2, and FLArE in Fig. 8. It is clear that FLArE (100 t) has the best sensitivity, followed by FASERν2, FLArE (10 t), and FASERν. Comparing the left (CC) and right (NC) results in Fig. 8, the sensitivities obtained using CC scattering are slightly better than those using NC scattering. This is because we have summed over all charged leptons in CC and all neutrino flavors in NC, and the CC suffers from the massive tau lepton in the phase space. Thus, the sensitivities using CC are only slightly better than those using NC. The sensitivity curves are also marginally better than that of the $g_U \times \beta^{12}$ curves shown in the middle panel of Fig. 7, since the muon (anti)neutrino and flux dominates over that of electron and tau neutrinos in the FPF detectors.

Finally, we can combine the number of signal events for both CC and NC scattering. The sensitivity curves for the overall coupling g_U are shown in Fig. 9. It clearly shows the improvement from the individual NC or CC result.

The sensitivity can reach down to 4×10^{-5} for the current FASERν in the sub-GeV leptoquark mass range. In the electroweak leptoquark mass range, the sensitivity lies in between 10^{-3} and 10^{-1}. For other proposed

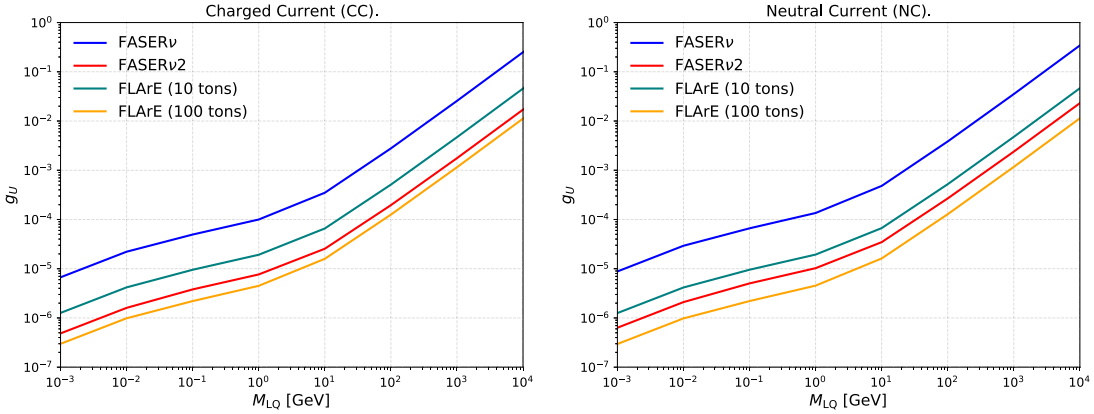

FIG. 8. 95% CL sensitivity curves on g_U for CC, $\nu_i + N \to l_j + N'$ (left panel); and NC, $\nu_i + N \to \nu_j + N'$ (right panel).

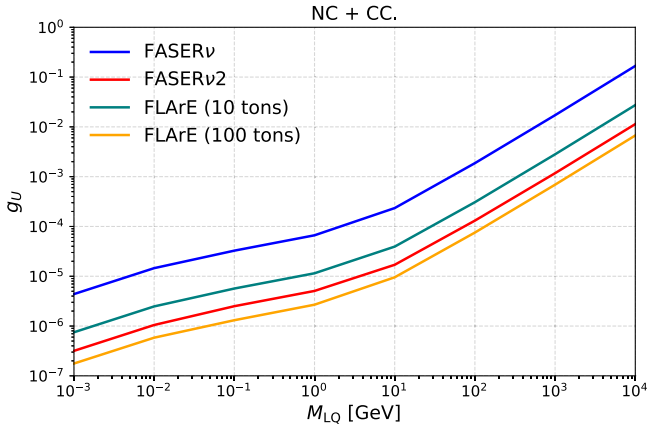

FIG. 9. 95% CL sensitivity curves on g_U when combining both CC and NC events.

detectors, the sensitivity can go down by 1 to 2 orders of magnitude. We can also compare the sensitivity of each FPF detector: FLArE 100 tons is the best, the next is the FASERν2, and then FLArE 10 tons.

In Figure 10, we compare our results to those in the literature, especially in the LQ mass range from 500 GeV to 2.5 TeV (in linear scale to match the mass region in [57,58]). In the left subfigure, the corresponding coupling ruled out by IceCube [59–62] is above 0.6–1.0 for the first-generation quark-lepton coupling in the 0.5–1 TeV mass range, while the bound from low-energy experiments [63] can go down to 0.2–0.8 for the 500–2500 GeV mass range. The LHC-13 TeV put a stringent limit for the LQ mass around 1600 GeV due to pair production, which is independent of the Yukawa couplings as long as they are not extremely small as the current search is based on prompt decays of the leptoquarks [64,65]. However, for LQ above 1.6 TeV the first-generation coupling is only excluded in the region above 0.7. In the right subfigure for the overall coupling, we show the lower mass limits of the leptoquark from both ATLAS [66] and CMS [67], and their projections for leptoquark-pair production, which exclude LQ masses below 1 TeV. We also included the bound from τ-pair production from [66] and its projection. For higher LQ masses around 2 TeV, the limits for each individual coupling can be pushed down to around 0.1, even smaller than the results from a recent study on SMEFT operators from the high-p_T tail in [68].

We overlay our results for FPF detectors in Fig. 10. For FASERν, the sensitivity can reach down to ~0.01 or $M_{U_1} = 500$ GeV to ~0.1 for $M_{U_1} = 2500$ GeV. Other FPF detectors, as we showed before, can achieve better sensitivities than FASERν. Such FPF experiments can probe the currently allowed regions and improve the constraints on the vector leptoquark model.

The sensitivity curves from FASERν are already better than those excluded regions by 1–2 orders of magnitude. Furthermore, the other FPF detectors can further improve the sensitivity by another 1–2 orders of magnitude in the TeV leptoquark mass range. In addition, the experiments proposed in FPF can probe a broad mass range of the leptoquark; especially, the FPF detectors are able to probe the region with small couplings in the sub-GeV leptoquark mass range, which is a challenge for the conventional hadron colliders.

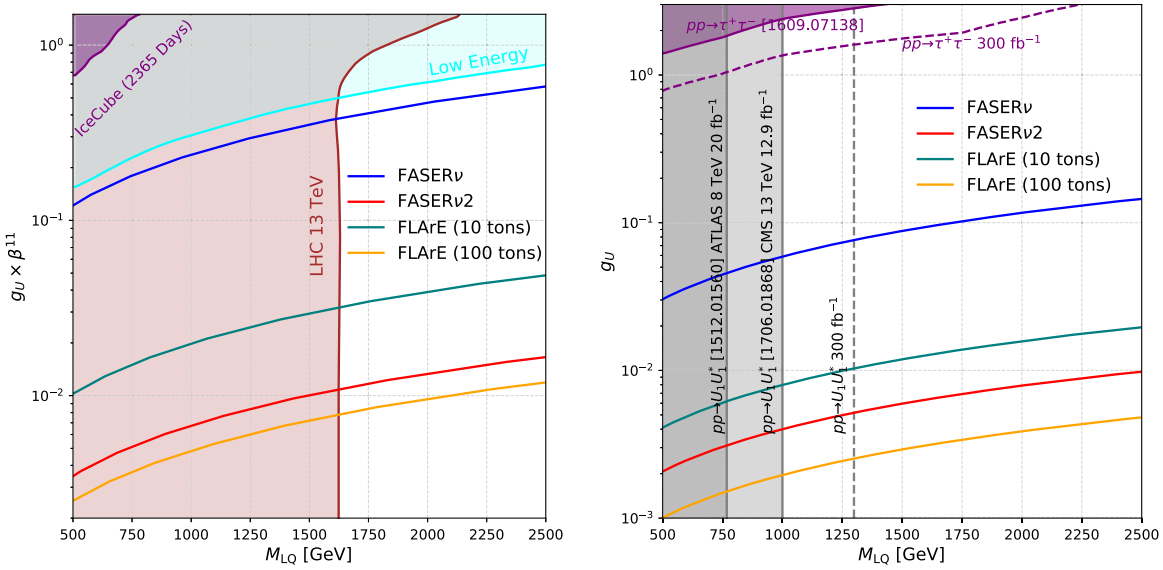

FIG. 10. Comparing the sensitivity reach from the FPF detectors with other constraints in the TeV regime. Left: excluded regions for the $g_U \times \beta^{11}$ from IceCube [59–62], LHC 13 TeV [69,70], and from low-energy experiments [63]. Right: bounds on the overall coupling g_U from ATLAS [66], CMS [67] for both LQ-pair and τ-pair [66] production, and the projection for High Luminosity LHC.

IV. CONCLUSIONS

The proposed Forward Physics Facility offers an array of experiments, which can take advantage of the unique neutrino beam in the energy range of a few hundred GeV to TeV to explore the physics beyond the SM. We have investigated the sensitivity reach on the leptoquark model at a number of experiments, including FASERν, FASERν2, FLArE(10 tons), and FLArE(100 tons). We compared the advantage of the FPF experiments in a wide mass range of the LQ mass to determine the flavor dependence of the couplings between the neutrinos and this LQ.

We have covered a wide mass range of LQ mass 10^{-3} GeV $\leq M_{LQ} \leq 10^{4}$ GeV in our study. Among all the proposed FPF experiments, FLArE(100 tons) has the best sensitivity to the LQ model, whereas FASERν has the least. The sensitivity curves for all the experiments follow a similar pattern, in which the sensitivity is weakened with the increment of the LQ mass. The unique feature of the LQ is that it contributes to both NC and CC-like neutrino-nucleon scattering at the FPF. We obtained the final sensitivities for the LQ couplings by combining both the CC and NC events.

ACKNOWLEDGMENTS

Special thanks to Felix Kling and Zeren Simon Wang for enlightening discussions. T. T. Q. N. would like to thank the Department of Physics and Center for Theory and Computation, NTHU, Taiwan for its hospitality. The work of T. T. Q. N. as a research assistant is supported in part by the Ministry of Science and Technology (MoST) of Taiwan under Grant No. 111-2112-M-001-035. K. C. and C. J. O. are supported by MoST under Grant No. 110-2112-M-007-017-MY3.

[1] R. Aaij *et al.* (LHCb Collaboration), Test of lepton universality in beauty-quark decays, Nat. Phys. **18**, 277 (2022).
[2] R. Aaij *et al.* (LHCb Collaboration), Test of lepton universality with $B^0 \to K^{*0}\ell^+\ell^-$ decays, J. High Energy Phys. 08 (2017) 055.
[3] LHCb Collaboration, Measurement of lepton universality parameters in $B^+ \to K^+\ell^+\ell^-$ and $B^0 \to K^{*0}\ell^+\ell^-$ decays, arXiv:2212.09153.
[4] Y. S. Amhis *et al.* (HFLAV Collaboration), Averages of b-hadron, c-hadron, and τ-lepton properties as of 2018, Eur. Phys. J. C **81**, 226 (2021).
[5] B. Abi *et al.* (Muon g-2 Collaboration), Measurement of the Positive Muon Anomalous Magnetic Moment to 0.46 ppm, Phys. Rev. Lett. **126**, 141801 (2021).
[6] S. Borsanyi *et al.*, Leading hadronic contribution to the muon magnetic moment from lattice QCD, Nature (London) **593**, 51 (2021).
[7] T. Blum, N. Christ, M. Hayakawa, T. Izubuchi, L. Jin, C. Jung, and C. Lehner, Hadronic Light-by-Light Scattering Contribution to the Muon Anomalous Magnetic Moment from Lattice QCD, Phys. Rev. Lett. **124**, 132002 (2020).
[8] L. Calibbi, A. Crivellin, and T. Ota, Effective Field Theory Approach to $b \to s\ell\ell^{(\prime)}$, $B \to K^{(*)}\nu\bar{\nu}$ and $B \to D^{(*)}\tau\nu$ with Third Generation Couplings, Phys. Rev. Lett. **115**, 181801 (2015).
[9] L. Calibbi, A. Crivellin, and T. Li, Model of vector leptoquarks in view of the B-physics anomalies, Phys. Rev. D **98**, 115002 (2018).
[10] A. Angelescu, D. Bečirević, D. A. Faroughy, F. Jaffredo, and O. Sumensari, Single leptoquark solutions to the B-physics anomalies, Phys. Rev. D **104**, 055017 (2021).
[11] K. Cheung, W.-Y. Keung, and P.-Y. Tseng, Isodoublet vector leptoquark solution to the muon $g-2$, $R_{K,K*}$, $R_{D,D*}$, and W-mass anomalies, Phys. Rev. D **106**, 015029 (2022).
[12] J. L. Feng *et al.*, The forward physics facility at the high-luminosity LHC, J. Phys. G **50**, 030501 (2023).
[13] D. Hayakawa, Poster by D. Hayakawa in NEUTRINO 2022, held in Seoul Korea, May 30—June 4.
[14] A. Crescenzo and F. Kling, Talk by A.Di Crescenzo and Felix Kling in NEUTRINO 2022, held in Seoul Korea, May 30—June 4.
[15] K. Cheung, C. J. Ouseph, and T. Wang, Non-standard neutrino and Z' interactions at the FASERν and the LHC, J. High Energy Phys. 12 (2021) 209.
[16] L. Di Luzio, J. Fuentes-Martin, A. Greljo, M. Nardecchia, and S. Renner, Maximal flavour violation: A Cabibbo mechanism for leptoquarks, J. High Energy Phys. 11 (2018) 081.
[17] M. J. Baker, J. Fuentes-Martín, G. Isidori, and M. König, High- p_T signatures in vector–leptoquark models, Eur. Phys. J. C **79**, 334 (2019).
[18] C. Cornella, D. A. Faroughy, J. Fuentes-Martin, G. Isidori, and M. Neubert, Reading the footprints of the B-meson flavor anomalies, J. High Energy Phys. 08 (2021) 050.
[19] A. Alloul, N. D. Christensen, C. Degrande, C. Duhr, and B. Fuks, FeynRules 2.0—A complete toolbox for tree-level phenomenology, Comput. Phys. Commun. **185**, 2250 (2014).
[20] C. Cornella, J. Fuentes-Martin, and G. Isidori, Revisiting the vector leptoquark explanation of the B-physics anomalies, J. High Energy Phys. 07 (2019) 168.
[21] L. A. Anchordoqui *et al.*, The forward physics facility: Sites, experiments, and physics potential, Phys. Rep. **968**, 1 (2022).
[22] A. Ariga *et al.* (FASER Collaboration), FASER: Forward search experiment at the LHC, arXiv:1901.04468.
[23] H. Abreu *et al.* (FASER Collaboration), The tracking detector of the FASER experiment, Nucl. Instrum. Methods Phys. Res., Sect. A **1034**, 166825 (2022).

[24] H. Abreu *et al.* (FASER Collaboration), The trigger and data acquisition system of the FASER experiment, J. Instrum. **16**, P12028 (2021).
[25] H. Abreu *et al.* (FASER Collaboration), Technical proposal: FASERnu, arXiv:2001.03073.
[26] A. Ariga *et al.* (FASER Collaboration), Technical proposal for FASER: Forward search experiment at the LHC, arXiv:1812.09139.
[27] A. Ismail, R. Mammen Abraham, and F. Kling, Neutral current neutrino interactions at FASERν, Phys. Rev. D **103**, 056014 (2021).
[28] S. Ansarifard and Y. Farzan, Neutral exotica at FASERν and SND@LHC, J. High Energy Phys. 02 (2022) 049.
[29] K. Jodłowski and S. Trojanowski, Neutrino beam-dump experiment with FASER at the LHC, J. High Energy Phys. 05 (2021) 191.
[30] J. L. Feng, I. Galon, F. Kling, and S. Trojanowski, Dark Higgs bosons at the forward search experiment, Phys. Rev. D **97**, 055034 (2018).
[31] F. Kling and S. Trojanowski, Heavy neutral leptons at FASER, Phys. Rev. D **97**, 095016 (2018).
[32] J. L. Feng, I. Galon, F. Kling, and S. Trojanowski, Axionlike particles at FASER: The LHC as a photon beam dump, Phys. Rev. D **98**, 055021 (2018).
[33] F. Deppisch, S. Kulkarni, and W. Liu, Heavy neutrino production via Z' at the lifetime frontier, Phys. Rev. D **100**, 035005 (2019).
[34] P. Bakhti, Y. Farzan, and S. Pascoli, Discovery potential of FASERν with contained vertex and through-going events, J. High Energy Phys. 04 (2021) 075.
[35] Y. Jho, J. Kim, P. Ko, and S. C. Park, Search for sterile neutrino with light gauge interactions: Recasting collider, beam-dump, and neutrino telescope searches, arXiv:2008.12598.
[36] N. Okada, S. Okada, and Q. Shafi, Light Z' and dark matter from $U(1)_X$ gauge symmetry, Phys. Lett. B **810**, 135845 (2020).
[37] M. Bahraminasr, P. Bakhti, and M. Rajaee, Sensitivities to secret neutrino interaction at FASERν, J. Phys. G **48**, 095001 (2021).
[38] K. J. Kelly, M. Sen, W. Tangarife, and Y. Zhang, Origin of sterile neutrino dark matter via secret neutrino interactions with vector bosons, Phys. Rev. D **101**, 115031 (2020).
[39] A. Falkowski, M. González-Alonso, J. Kopp, Y. Soreq, and Z. Tabrizi, EFT at FASERν, J. High Energy Phys. 10 (2021) 086.
[40] A. Ariga *et al.* (FASER Collaboration), FASER's physics reach for long-lived particles, Phys. Rev. D **99**, 095011 (2019).
[41] K. Asai, A. Das, J. Li, T. Nomura, and O. Seto, Chiral Z' in FASER, FASER2, DUNE, and ILC beam dump experiments, Phys. Rev. D **106**, 095033 (2022).
[42] G. Cottin, J. C. Helo, M. Hirsch, A. Titov, and Z. S. Wang, Heavy neutral leptons in effective field theory and the high-luminosity LHC, J. High Energy Phys. 09 (2021) 039.
[43] A. Ismail, S. Jana, and R. M. Abraham, Neutrino upscattering via the dipole portal at forward LHC detectors, Phys. Rev. D **105**, 055008 (2022).
[44] B. Batell, J. L. Feng, A. Ismail, F. Kling, R. M. Abraham, and S. Trojanowski, Discovering dark matter at the LHC through its nuclear scattering in far-forward emulsion and liquid argon detectors, Phys. Rev. D **104**, 035036 (2021).
[45] B. Batell, J. L. Feng, M. Fieg, A. Ismail, F. Kling, R. M. Abraham, and S. Trojanowski, Hadrophilic dark sectors at the forward physics facility, Phys. Rev. D **105**, 075001 (2022).
[46] K. Cheung and C. J. Ouseph, Sensitivities on dark photon from the forward physics experiments, J. High Energy Phys. 10 (2022) 196.
[47] K. Cheung and C. J. Ouseph, Constraining the active-to-heavy-neutrino transitional magnetic moments associated with the Z' interactions at FASERν, Eur. Phys. J. C **83**, 593 (2023).
[48] D. Aloni and A. Dery, Revisiting leptonic non-unitarity in light of FASERν, arXiv:2211.09638.
[49] J. Arakawa, J. L. Feng, A. Ismail, F. Kling, and M. Waterbury, Neutrino detection without neutrino detectors: Discovering collider neutrinos at FASER with electronic signals only, Phys. Rev. D **106**, 052011 (2022).
[50] H. Abreu *et al.* (FASER Collaboration), Detecting and studying high-energy collider neutrinos with FASER at the LHC, Eur. Phys. J. C **80**, 61 (2020).
[51] A. Buckley, J. Ferrando, S. Lloyd, K. Nordström, B. Page, M. Rüfenacht, M. Schönherr, and G. Watt, LHAPDF6: Parton density access in the LHC precision era, Eur. Phys. J. C **75**, 132 (2015).
[52] J. Alwall, R. Frederix, S. Frixione, V. Hirschi, F. Maltoni, O. Mattelaer, H. S. Shao, T. Stelzer, P. Torrielli, and M. Zaro, The automated computation of tree-level and next-to-leading order differential cross sections, and their matching to parton shower simulations, J. High Energy Phys. 07 (2014) 079.
[53] J. Alwall, M. Herquet, F. Maltoni, O. Mattelaer, and T. Stelzer, MadGraph 5: Going beyond, J. High Energy Phys. 06 (2011) 128.
[54] R. D. Ball *et al.* (NNPDF Collaboration), Parton distributions from high-precision collider data, Eur. Phys. J. C **77**, 663 (2017).
[55] F. Kling and L. J. Nevay, Forward neutrino fluxes at the LHC, Phys. Rev. D **104**, 113008 (2021).
[56] P. Ballett, M. Hostert, S. Pascoli, Y. F. Perez-Gonzalez, Z. Tabrizi, and R. Zukanovich Funchal, Z's in neutrino scattering at DUNE, Phys. Rev. D **100**, 055012 (2019).
[57] I. Doršner, S. Fajfer, and M. Patra, A comparative study of the S_1 and U_1 leptoquark effects in the light quark regime, Eur. Phys. J. C **80**, 204 (2020).
[58] D. Buttazzo, A. Greljo, G. Isidori, and D. Marzocca, B-physics anomalies: A guide to combined explanations, J. High Energy Phys. 11 (2017) 044.
[59] M. G. Aartsen *et al.* (IceCube Collaboration), Evidence for high-energy extraterrestrial neutrinos at the IceCube detector, Science **342**, 1242856 (2013).
[60] M. G. Aartsen *et al.* (IceCube Collaboration), Observation of High-Energy Astrophysical Neutrinos in Three Years of IceCube Data, Phys. Rev. Lett. **113**, 101101 (2014).

[61] M. G. Aartsen *et al.* (IceCube Collaboration), The IceCube neutrino observatory—contributions to ICRC 2017 part II: Properties of the atmospheric and astrophysical neutrino flux, arXiv:1710.01191.

[62] A. Schneider (IceCube Collaboration), Characterization of the astrophysical diffuse neutrino flux with IceCube high-energy starting events, *Proc. Sci.*, ICRC2019 (2020) 1004 [arXiv:1907.11266].

[63] P. Arnan, D. Becirevic, F. Mescia, and O. Sumensari, Probing low energy scalar leptoquarks by the leptonic W and Z couplings, J. High Energy Phys. 02 (2019) 109.

[64] B. Diaz, M. Schmaltz, and Y.-M. Zhong, The leptoquark Hunter's guide: Pair production, J. High Energy Phys. 10 (2017) 097.

[65] M. Schmaltz and Y.-M. Zhong, The leptoquark Hunter's guide: Large coupling, J. High Energy Phys. 01 (2019) 132.

[66] D. A. Faroughy, A. Greljo, and J. F. Kamenik, Confronting lepton flavor universality violation in B decays with high-p_T tau lepton searches at LHC, Phys. Lett. B **764**, 126 (2017).

[67] L. Di Luzio and M. Nardecchia, What is the scale of new physics behind the B-flavour anomalies?, Eur. Phys. J. C **77**, 536 (2017).

[68] L. Allwicher, D. A. Faroughy, F. Jaffredo, O. Sumensari, and F. Wilsch, Drell-Yan tails beyond the standard model, J. High Energy Phys. 03 (2023) 064.

[69] M. Aaboud *et al.* (ATLAS Collaboration), Search for scalar leptoquarks in pp collisions at $\sqrt{s} = 13$ TeV with the ATLAS experiment, New J. Phys. **18**, 093016 (2016).

[70] V. Khachatryan *et al.* (CMS Collaboration), Search for single production of scalar leptoquarks in proton-proton collisions at $\sqrt{s} = 8$ TeV, Phys. Rev. D **93**, 032005 (2016); **95**, 039906(E) (2017).